Domain-Wall Guided Nucleation of Superconductivity in Hybrid Ferromagnet-Superconductor-Ferromagnet Layered Structures

W. Gillijns,[1,*] A. Yu. Aladyshkin,[1,2] M. Lange,[1,†] M. J. Van Bael,[1] and V. V. Moshchalkov[1]

[1]*INPAC–Institute for Nanoscale Physics and Chemistry, Nanoscale Superconductivity and Magnetism Group, K.U. Leuven, Celestijnenlaan 200D, B-3001 Leuven, Belgium*

[2]*Institute for Physics of Microstructures RAS, 603950, Nizhny Novgorod, GSP-105, Russia*

(Received 16 June 2005; published 21 November 2005)

Domain-wall superconductivity is studied in a superconducting Nb film placed between two ferromagnetic Co/Pd multilayers with perpendicular magnetization. The parameters of top and bottom ferromagnetic films are chosen to provide different coercive fields, so that the magnetic domain structure of the ferromagnets can be selectively controlled. From the dependence of the critical temperature T_c on the applied magnetic field H, we have found evidence for domain-wall superconductivity in this three-layered F/S/F structure for different magnetic domain patterns. The phase boundary, calculated numerically for this structure from the linearized Ginzburg-Landau equation, is in good agreement with the experimental data.

DOI: 10.1103/PhysRevLett.95.227003 PACS numbers: 74.78.Fk, 74.25.Dw, 74.25.Op, 74.78.Na

Superconductivity (S) and ferromagnetism (F) have long been known to be antagonistic phenomena. This is a result of the pair breaking effects in superconductors due to the electromagnetic and the exchange interactions. A lot of effort has been devoted to the experimental and theoretical investigations of the properties of ferromagnetic superconductors and S/F-hybrid structures (see Refs. [1–4], and references therein). In these structures, a rich variety of interesting phenomena have been observed. The electromagnetic interaction significantly changes the superconducting properties due to the inhomogeneous stray fields, induced by the ferromagnet, in the superconductor. These stray fields can be created by magnetic nanostructures such as dots [5–7] and films [8]. In S/F bilayers, the domain structure in the F film with out-of-plane magnetization leads to so-called domain-wall superconductivity (DWS) [8]. Recently, DWS was also experimentally observed in S/F bilayers with in-plane magnetization [9]. In this case, it is a result from the proximity effect and the reduced exchange field at the domain wall [10].

Neglecting the exchange interaction and taking only the electromagnetic interaction into account, DWS was studied in S/F bilayers for a one-dimensional (1D) static domain structure [11]. Because of the nonuniformity of the stray field of the F film, positions where the perpendicular component of the total magnetic field is close to zero become energetically favorable for superconductivity to nucleate. In an S/F *bilayer* with a *thick* F film, Yang *et al.* [8] observed an increase of the critical temperature T_c with increasing external magnetic field H near $H = 0$. This reentrant behavior was predicted by theory in the thick F-film case [11]. But, since the domains moved reversibly during the field sweep, only a qualitative comparison could be made.

In this Letter, we investigate the nucleation of superconductivity in a planar *thin-film*, *three*-layered F/S/F hybrid. Using 2 F layers, different magnetic configurations can be obtained in contrast to a system with 1 F layer. In this way, the influence of different field distributions on the superconductor can be investigated in one sample. First, the amplitude of modulation of the stray field in this system can be controlled due to the superposition of the two individual stray fields of both F films; thus, the dependence of the phase boundary on the amplitude of modulation can be investigated. Second, a relative shift between the domain structure in both F films results in positions at which the stray field is close to zero, and, hence, one can expect that the nucleation of superconductivity will be favored at these positions. These F/S/F trilayers, therefore, provide new possibilities to tune the superconducting properties by using magnetic templates. The interest in the *thin F-film* bilayers and trilayers is also stimulated by the fact that the theory of the superconducting nucleation in such systems considered only an isolated domain wall in the thin F layer. It was shown that reentrant behavior is absent in this case [11]. Thus, the question whether the reentrance of superconductivity could be realized in thin-film S/F and F/S/F hybrids with a *regular domain structure* remains unanswered. Keeping the applied field lower than the coercive fields of the F films, we have a fixed magnetic domain distribution, and, hence, we can interpret the nucleation of superconductivity in our samples accurately within a model similar to the one in Ref. [11], taking into account the particular nonuniform field distribution of thin F films.

Our F/S/F trilayer consists of a superconducting Nb film with a thickness of $D_s = 35$ nm, sandwiched between two ferromagnetic Co/Pd multilayered films. The sample was prepared by molecular beam epitaxy deposition and has a lateral size of about 3×3 mm^2. The ''top'' and ''bottom'' Co/Pd multilayers consist of ten bilayers of Co (0.4 nm) and Pd (1.5 and 1.2 nm in the top and bottom films, respectively) on top of a Pd base layer (again 1.5 and 1.2 nm in top and bottom). Such Co/Pd multilayers are known to possess perpendicular magnetic anisotropy [12].

The hysteresis loop of the F/S/F structure was measured in a SQUID magnetometer in a perpendicular applied field at $T = 6$ K (above the critical temperature of our sample) and is shown in Fig. 1. The different Pd thickness in the top and bottom Co/Pd films results in a higher coercive field of the top -film ($H_{\mathrm{coer}}^{\mathrm{top}} \simeq 480$ mT) with respect to the bottom F film ($H_{\mathrm{coer}}^{\mathrm{bot}} \simeq 380$ mT). As a result, different magnetic states of the F/S/F structure can be achieved. In order to study DWS, we are especially interested in those states in which (i) both F films are fully magnetized (MM), (ii) one F film (top) is magnetized while the other (bottom) is demagnetized and is split into domains (zero net magnetization) (DM), and (iii) both F films are demagnetized (DD). The MM state is the remanent state after magnetizing the sample in 1 T. The DD state is obtained by oscillating the field to zero, starting from 1 T (above the coercive fields of both F films). Finally, to achieve the DM state, both F films are first saturated in 1 T after which the field is oscillated to zero, this time starting from a field between the coercive fields of both films. This will demagnetize only the bottom F film, while the top F film remains magnetized.

Figure 2 shows the magnetic force microscopy (MFM) images ($T = 300$ K) for the DM and DD states. In Fig. 2(a) (DM), the bright and dark contrast results from the positive and negative domains in the bottom F film (''2-color template''). A more complicated picture with different color levels is obtained in the DD state [Figs. 2(b) and 2(c)]. The combination of the domains in the top and bottom F films yields four possible orientations, as indicated in Fig. 2(c): The darkest (1) [brightest (4)] regions occur where the magnetizations in both F films are parallel and negative (positive). Regions where the magnetizations in both F films are opposite correspond to the intermediate contrasts (2 and 3). Of these two, the darker (2) [lighter (3)] can be associated with regions where the magnetization is negative (positive) in the top film and positive (negative) in the bottom film. Note that the last two regions are equivalent for the superconductor, and, hence, we have obtained a 3-color template in the DD case. The domains are elongated in shape and their typical width ranges from 200 (transverse direction) to 800 nm (longitudinal direction).

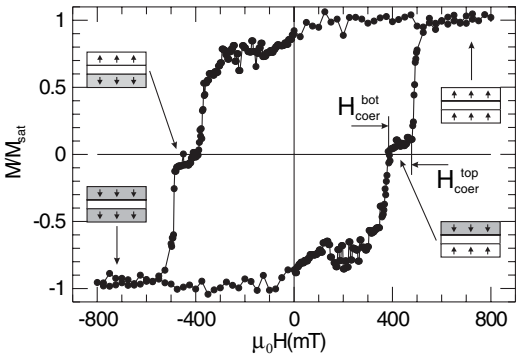

FIG. 1. Magnetization loop of the F/S/F three-layered structure at 6 K, $M_{\mathrm{sat}} = 1.89 \times 10^{-4}$ emu. Note the difference in coercive field of the top (~480 mT) and the bottom (~380 mT) layers.

We have carried out measurements of the electrical resistivity ρ of the F/S/F structures in a standard four probe geometry in different magnetic states (MM, DM, DD) as a function of temperature T and external magnetic field H, which was oriented perpendicular to the sample surface and was kept lower than the coercive fields of both F films. Using the measured dependencies $\rho(T)$ at constant H, the phase boundary $T_c(H)$ was reconstructed. The critical temperature T_c was defined as the temperature at which the resistance was 50% of the normal state resistance [i.e., $R(T_c) = 0.5R_N$]. The phase transition lines $T_c(H)$ for the F/S/F structure in the DM and DD states are shown in Figs. 3(a) and 3(b), respectively, together with the MM state. The phase boundary $T_c(H)$ is found to be strongly dependent on the spatial distribution of the magnetic field induced by the ferromagnets similar to the S/F hybrids with thick F film (see Refs. [8,11,13]).

The linear dependence of $T_c(H)$ in the MM configuration is similar to that of a large-area simply connected superconductor in an uniform magnetic field [△ in Figs. 3(a) and 3(b)]. This can be understood since the stray field of a uniformly magnetized F film is close to zero (except at the sample edges) and, hence, does not magnetically affect the S film.

The phase boundary in the DM state, where only 1 F layer is magnetically active [□ in Fig. 3(a)], demonstrates reentrant behavior: At low fields ($|H| < 18$ mT) the critical temperature T_c increases by increasing $|H|$ and reaches a maximum at about $H_{\mathrm{max}}^{\mathrm{DM}} \simeq \pm 18$ mT. Further increasing the field results in a suppression of the critical temperature. Thus, even for the thin F layer configuration, reentrant behavior is present. An applied field compensates the field of the oppositely oriented domains and lowers the total field at these domains. Thus, the critical temperature increases until these domains are optimally compensated. Further increasing the field will overcompensate the domains, and, hence, T_c will decrease. The phase boundary in the DD state, where both F layers are ''switched on'' [○ in Fig. 3(b)], exhibits a similar shape. There are, however, differences: (i) The compensation field (field at which the

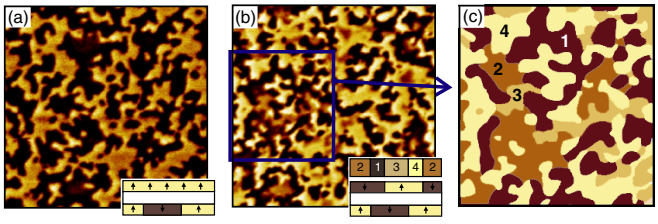

FIG. 2 (color online). (a) 10×10 μm^2 MFM image of the F/S/F structure in the DM state. (b) 10×10 μm^2 MFM image in the DD state. (c) 5×5 μm^2 schematical drawing of the area from panel (b). The four different configurations are numbered (1–4). The insets show a schematic drawing of the appropriate magnetic configurations.

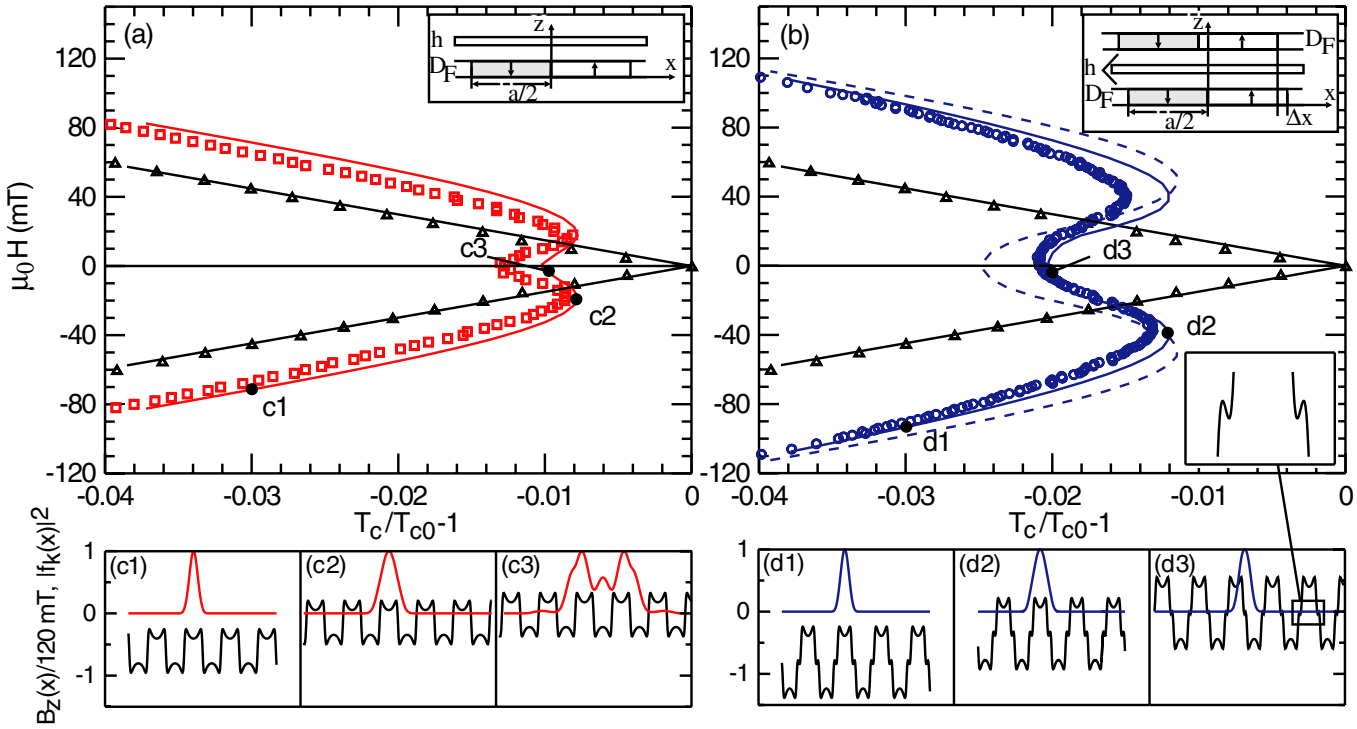

FIG. 3 (color online). (a) Experimental phase boundaries $T_c(H)$ in the MM state (△) and in the DM state (□) and the calculated phase boundaries (solid lines); (b) experimental phase boundaries $T_c(H)$ in the MM state (△) and in the DD state (○) and calculated phase boundaries for $\Delta x = 0$ (dashed blue line) and $\Delta x = 0.125a$ (solid blue line). Upper insets in (a),(b) represent the model used for the description of the DM and DD states. Lower inset in (b) shows the spatial structure of the magnetic field near the domain wall in the DD state for $\Delta x = 0.125a$. (c) and (d) The total magnetic field distribution $B_z(x) = \mu_0 H + b_z(x)$ and the OP distribution $|f_k(x)|^2$ for the DM state and the DD state ($\Delta x = 0.125a$), respectively.

maximal value of T_c is reached) $H_{\max}^{\mathrm{DD}} \simeq 38$ mT is about twice as large as $H_{\max}^{\mathrm{DM}}$; and (ii) T_c is higher in the high field limit and lower in the low field regime.

To better understand the superconducting nucleation, we use a simple theoretical model, based on the linearized Ginzburg-Landau equation (see details in Ref. [11]). Taking into account the electromagnetic mechanism only, we consider the nucleation in a thin S film in a 1D magnetic field profile $B_z(x) = \mu_0 H + b_z(x)$, where the component $b_z(x)$ is induced by the two thin F films (the orientation of the axes is shown in the upper insets in Fig. 3). We seek the spatial distribution of the order parameter (OP) in the form: $\psi(x, y) = f_k(x)e^{iky}$. We have assumed the following distributions of the magnetization: $M^{\mathrm{bot}}(x) = M_0 \mathrm{sgn}(x)$ for $|x| < a/2$ and $M^{\mathrm{bot}}(x + na) = M^{\mathrm{bot}}(x)$, $M^{\mathrm{top}}(x) = M^{\mathrm{bot}}(x + \Delta x)$, where a is the period of the domain structures, n is the integer, M_0 is the amplitude of the magnetization, and Δx is the mutual shift between domain structures in the 2 F films. For the calculation of the magnetic field distribution $b_z(x)$, we use the analytical expression given in Ref. [14]. A nonzero distance $h \sim D_s/2$ between the S film and the F films allows us to take into account the suppression of superconductivity near the S/F interface due to the proximity effect. Thus, there are five variable parameters in our model: M_0, a, Δx, the critical temperature of the S film T_{c0} in the absence of the magnetic field, and the coherence length ξ_0; the thickness of the F films $D_F \simeq 17.5$ nm and $h \simeq 17.5$ nm is fixed.

The phase boundaries $T_c(H)$, obtained from the numerical calculations, are shown in Fig. 3 as lines. The appropriate values for $T_{c0} = 4.78$ K and $\xi_0 = 14.5$ nm are determined from the approximation of the experimental data for the MM case [Fig. 3(a)]. The dependence $T_c(H)$ for the DM state, calculated for reasonable parameters $M_0 = 3 \times 10^5$ A/m and $a = 30D_F$, is shown in Fig. 3(a). The dependencies $T_c(H)$ for the DD state, calculated for the same parameters M_0 and a and for $\Delta x = 0$ (dashed line) and for $\Delta x = 0.125a$ (solid line), are presented in Fig. 3(b). The profiles of the total field $B_z(x)$ and the OP $|f_k(x)|^2$ for the different values of H are presented in Fig. 3(c) for the DM case and in Fig. 3(d) for the DD case ($\Delta x = 0.125a$).

This simple model gives nice qualitative and quite good quantitative agreement with the experimental data. The best fits were obtained for a half-period $a/2 = 262$ nm. This indicates that the shortest side of the domains mainly determines the phase boundary in our sample. Strictly speaking, the proximity effect and the exchange interaction cannot be neglected in our F/S/F system without an insulating barrier. However, one can see that the proximity effect will result only in a global reduction of T_c and will have no apparent effect on the shape of the phase boundary.

The differences between the DM and the DD states can be explained by considering that the amplitude of modulation differs approximately by a factor of 2 in both cases. The difference in compensation fields in DM and DD states is a direct consequence of this. The double stray field in the DD case results in the fact that the field needed for optimum compensation is also double. In the low field limit ($|H| \leq H_{\max}^{\mathrm{DM}}$), the higher critical temperature in the DM state can be explained by noting that the suppression of the T_c due to the orbital effect is $\Delta T_c^{\mathrm{orb}} \sim T_{c0}\bar{b}/H_{c2}(0)$, where $H_{c2}(0) = \Phi_0/(2\pi\xi_0^2)$ is the upper critical field and $\bar{b}$ is the typical field $|b_z(x)|$ inside the domain. Thus, the smaller the amplitude of modulation b_z, the smaller the suppression of the critical temperature $\Delta T_c^{\mathrm{orb}}$ and, correspondingly, the higher T_c. In the high field limit ($|H| > H_{\max}^{\mathrm{DD}}$), however, superconductivity nucleates near the minimum of the total field $|\mu_0 H + b_z(x)|$ [see Figs. 3(c) and 3(d), panels (c1) and (d1)]. Thus, the higher amplitude of $b_z(x)$ in the DD case will lead to a lower total field at these positions and, hence, a higher critical temperature in the high field limit. Note that the phase boundary is broadened significantly in the high field limit, depending on the magnitude of the magnetization.

The OP itself is also strongly influenced by the modulation amplitude. In the low field limit, there is a wide superconducting nucleus for the DM state and well localized nucleus for the DD state [compare Figs. 3(c) and 3(d), panels (c3) and (d3)]. This distinction can be explained by the fact that the typical width L of the superconducting OP in a uniform field b_0 is determined as follows: $L = \sqrt{\Phi_0/2\pi b_0}$, where Φ_0 is the flux quantum. Substituting $\bar{b}$ for b_0, one gets the estimates of $L^{\mathrm{DM}} \simeq 100$ nm and $L^{\mathrm{DD}} \simeq 70$ nm. Since the important length scale of the domains is about 200 nm in both cases, one can expect that in the DD case the nonuniform field $b_z(x)$ gives rise to an effective decay of the OP inside the domain, contrary to the OP in the DM case. Thus, the difference in amplitude of b_z is the cause of the *crossover from a localized to a nonlocalized OP profile*.

Another important difference between the 2-color and 3-color templates is the appearance of regions with opposite magnetization (3rd color) as a consequence of the relative shift Δx. The increase in Δx results in the appearance of regions where $b_z(x)$ is close to zero [see lower inset in Fig. 3(b)]. On one hand, these regions stimulate the nucleation of superconductivity near the domain walls and enhance T_c in the low field regime [compare the dashed and solid lines in Fig. 3(b)]. On the other hand, the difference between the maximal T_c and $T_c(H = 0)$ decreases with increasing Δx, and, hence, the reentrant behavior becomes less pronounced.

Our calculations confirm that the asymmetry $T_c(H) \neq T_c(-H)$ [Fig. 3(b)] can be explained by a small difference in the width of the positive and negative domains (e.g., due to a nonperfect demagnetization procedure). One can intuitively expect that the critical temperature will depend on the confinement of the OP, similar to the dependence of the energy of a "particle in a box" on the width of the box. Since the sign of H determines whether the order parameter is located in the wide or narrow domains, it is also responsible for the higher or lower critical temperature, respectively, near the compensation field.

In conclusion, a thin-film, three-layered F/S/F structure was investigated both theoretically and experimentally. By using a three-layered F/S/F structure, different magnetic states and, hence, different magnetic field templates have been obtained. Reentrant behavior was found in this *thin* F-film hybrid structure. A direct comparison has been made between our experimental data and the model describing the nucleation of superconductivity for a fixed magnetic landscape. We found that this model describes the superconducting nucleation in the real hybrid F/S/F samples very well; i.e., our interpretation of the results in terms of domain-wall guided superconductivity is justified. By increasing the amplitude of modulation, the critical temperature will decrease in the low field limit and increase in the high field limit. The relative shift between the two domain structures artificially broadens the domain walls and, hence, facilitates the nucleation of superconductivity in the low field limit.

The authors are thankful to B. Opperdoes for help with sample preparation and to D. A. Ryzhov for help with programming. This work was supported by the K.U. Leuven Research Fund GOA/2004/2 program, the Belgian IUAP, and by the Fund for Scientific Research Flanders (Belgium) (F.W.O.-Vlaanderen). A. Yu. A. is supported by BELSPO Foundation, RFBR (Grant No. 03-02-16774) and by the Russian Ministry of Science and Education.

*Electronic address: werner.gillijns@fys.kuleuven.be
†Present address: NV Bekaert SA, Bekaertstraat 2, B-8550 Zwevegem, Belgium.

[1] J. Flouquet and A. Buzdin, Phys. World **15**, 41 (2002).
[2] I. F. Lyuksyutov and V. L. Pokrovsky, Adv. Phys. **54**, 67 (2005).
[3] Yu. A. Izyumov, Yu. N. Proshin, and M. G. Khusainov, Phys. Usp. **45**, 109 (2002).
[4] L. Lazar *et al.*, Phys. Rev. B **61**, 3711 (2000).
[5] M. Lange *et al.*, Phys. Rev. Lett. **90**, 197006 (2003).
[6] D. Stamopoulos, M. Pissas, and E. Manios, Phys. Rev. B **71**, 014522 (2005).
[7] D. S. Golubovic *et al.*, Appl. Phys. Lett. **83**, 1593 (2003).
[8] Z. Yang *et al.*, Nat. Mater. **3**, 793 (2004).
[9] A. Y. Rusanov, M. Hesselberth, J. Aarts, and A. I. Buzdin, Phys. Rev. Lett. **93**, 057002 (2004).
[10] A. I. Buzdin, L. N. Bulaevskii, and S. V. Panyukov, Sov. Phys. JETP **60**, 174 (1984).
[11] A. Yu. Aladyshkin *et al.*, Phys. Rev. B **68**, 184508 (2003).
[12] W. B. Zeper *et al.*, J. Appl. Phys. **65**, 4971 (1989).
[13] A. I. Buzdin and A. S. Mel'nikov, Phys. Rev. B **67**, 020503(R) (2003).
[14] E. B. Sonin, Phys. Rev. B **66**, 136501 (2002).